

Laser remote sensor for oil palm fruit ripeness assessment

Kok-Sing Lim¹, Batrisyia Ahmad Nazri², Wan Rusydiah Rusik², Amirul Al Hafiz Abdul Hamid³,
Cheong-Weng Ooi¹, Waldo Udos¹, Mohd Shiraz Aris³, Mohd Zulfahmi Mohd Yusof³,
Harikrishna Kulaveerasingam², Wu-Yi Chong¹, Mohamad Faizal Ismail¹ and Harith Ahmad¹

¹Photonics Research Centre, University of Malaya, 50603 Kuala Lumpur, Malaysia;

²Sime Darby Plantation Research Sdn Bhd, Jalan Banting-Kelanang, Simpang Sungai Arak, 42700
Banting, Selangor

³Sime Darby Plantation Research Sdn Bhd, Lot 2664, Jalan Pulau Carey, 42960 Pulau Carey,
Selangor

ABSTRACT

The color change of oil palm fresh fruit bunches (FFB) is one of the important parameters for harvesting decisions. However, human visual identification is prone to errors due to uncontrolled ambient lighting and the far distance of fruit bunches on tall palm trees. These errors can lead to inaccurate harvesting and significant revenue loss. This study introduces a laser remote sensor for non-destructive FFB ripeness assessment. Based on the unique spectral reflection curves of the FFB at different ripeness, laser modules at three different wavelengths (visible- NIR region) have been employed for the measurement. The photodetector and laser sources are configured in a coaxial manner to enable long work distances up to 9m. This portable laser remote sensor has undergone successful on-plant testing in oil palm estates, with measurements validated against oil content by conventional bunch analysis. It is a potential tool for precision harvesting and oil yield prediction.

Keywords: oil palm fruit, ripeness assessment, reflectance, remote sensing, near-infrared

1. INTRODUCTION

The fruit's appearance and colours are the widely used indicators for the assessment of fruit ripeness, quality and acceptability by farmers and consumers. The apparent reason is the fast and non-destructive nature of the method to gauge the optimal time for harvest and yields. For some fruits, there are clear correlations between the physical appearance (colours and shape) and biological condition (changing concentrations of pigments such as chlorophylls and carotenoids) in the epidermis layer of the fruits at different stages of ripeness. However, the conventional approach that relies on visual inspection is akin to a qualitative assessment in which the accuracy is highly dependent on the harvester's experience. Hence it is restricted to a small number of simple classifications (e.g. unripe, underripe, ripe and overripe) for the fruit assessment. Furthermore, the ambient lighting condition and the distance between the target fruit are critical parameters influencing the accuracy of the assessment.

Various non-destructive techniques for quantitative assessments have been proposed for instance colorimetry [1], visible imaging [2], visible and near-infrared (VNIR) spectroscopy [3], and hyperspectral imaging [4,5]. In the context of oil palm fruit assessments, the visible imaging technique based on the Red-Green-Blue (RGB) photos [6-8] captured by the standard cameras is a widely explored technique. There are other research efforts in exploring the visible-infrared spectrum of the oil palm fruit using the spectrometer or hyperspectral imaging device. A wider reflectance spectrum (400nm-1100nm) can provide more comprehensive information about the ripeness. The data from the near-infrared region (> 800nm) have also been explored and proven to be useful in the ripeness assessment for oil palm fruit [9,10].

A suitable light source with a broad spectrum is essential for the measurement. However, the low coherence property of broadband light makes it less ideal for remote sensing/measurement. Multi-band assessment techniques that are based on the LED sources at specific wavelengths have been suggested [11,12]. The work distance is limited (< 1m) and technically impractical for on-site operation and on-plant assessment.

2. THE SPECTRAL CHARACTERISTICS OF FRESH FRUIT BUNCH

Laser remote sensor is an enhanced version of a multiband sensor that employs lasers for long work distances (remote sensing). A laser is a coherent light source that can be collimated for illumination of the target at a further distance. The laser beam can be expanded using a beam expander so that the illuminating area of the fruit bunch can be controlled, and a more homogeneous measurement can be achieved. The laser power is scalable and controlled electronically according to the condition and this property is useful for the cancellation/elimination of noise in the detected signal by the photodetector. In the selection of laser wavelengths, the main consideration would be based on the good correlation between the reflectance and fruit ripeness as well as the minimum interference from the natural light.

Visible imaging technique based RGB photos captured by standard camera is probably the most widely explored technique for fruit ripeness assessment. The relationship between the captured RGB intensities from the photo and optical reflection spectrum of the fruit samples are not well understood. In this current study, a comparative study is performed.



Fig. 1. Illustrative diagram of the UV-Vis spectrometry measurement.

Fig. 1 illustrates the experimental setup for the UV-Vis spectrometry test using a spectrometer with a detection range from 200-1100nm. Halogen lamp is used as the illuminating light source for the measurement.

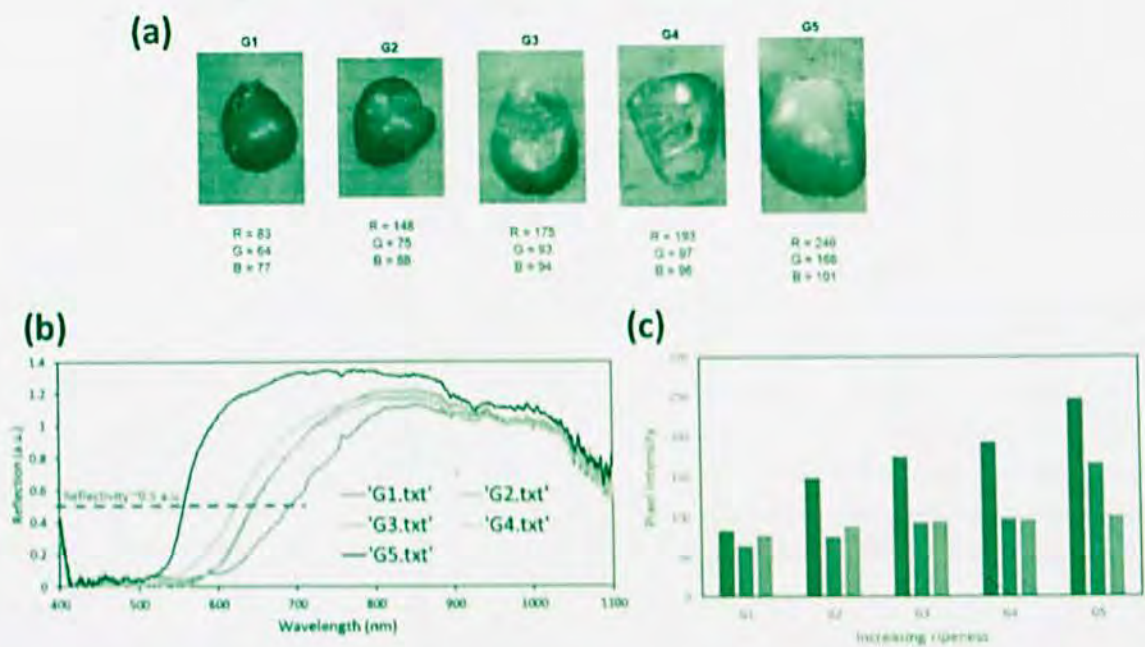


Fig. 2. Five oil palm fruit samples (slices) with different colours/ripeness were prepared and characterized.

Fig. 2(a) depicts the fruitlet specimens utilized in the characterization test. The small fractions of the fruitlet surface of varying ripeness (colours) were excised and employed in the investigative study. The fruitlet ripeness followed the sequence $G1 < G2 < G3 < G4 < G5$, transitioning from a dark purple to red orange as ripeness progressed. The corresponding reflection spectrum of each fruitlet to three ripeness stages were presented in Fig. 2(b).

The bandwidth of the reflection curve widened alongside ripening. The cutoff at the shorter wavelength region, which depicted as red straight line in Fig. 2(b) started at 700nm for G1, progressed to 640nm as the ripeness increased (from G2, G3, then G4) and eventually stopped at 560nm for G5. The reflectivity within the blue region (400 – 450nm) consistently low irrespective of ripeness, elucidating the low intensity observed in blue pixels and their limited correlation with fruit ripeness.

Fig. 2(c) shows the detected RGB pixel intensities that correspond to different ripeness levels. A good correlation was clearly shown between the intensity of red colour pixel and the level of ripeness, whereas the green and blue pixels do not exhibit any significant variation for sample G2, G3, and G4, with the blue pixel displayed the least discernible alterations. It was worth noting that the reflective spectrum exhibited an incremental pattern with increasing ripeness, with the sole intensity changes noticeable between G1 and G2.

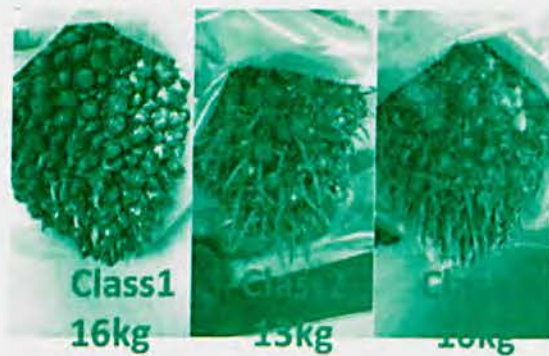


Fig. 3. FFBs at different levels of ripeness are characterized. From left to right: Unripe, Underripe and ripe.

The characterization test proceeded to three FFBs of different ripeness, classified as unripe, underripe, and ripe as shown in Fig. 3. The three FFBs were characterized using a halogen lamp and the reflection spectra of the bunches were recorded and measured via spectrometer. 6 – 8 sets of measurements were taken across various sections of the fruit bunches, and the spectral curves were averaged to produce a singular representative curve for each class of ripeness as shown in Fig. 4.

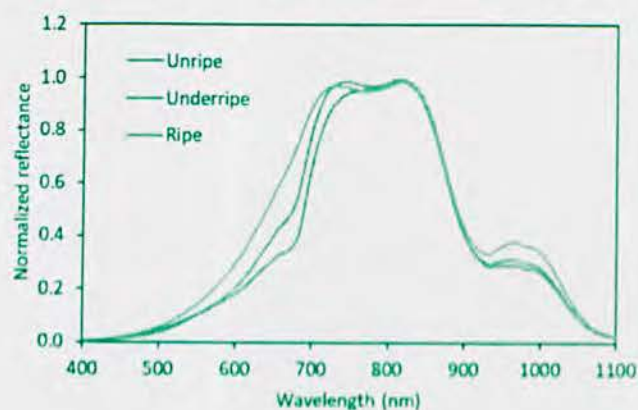


Fig. 4. The averaged reflection curves of FFBs (Unripe, Underripe, Ripe)

The analysis revealed that the spectral curve within the region of 570 – 750nm was sensitive to the change of ripeness, while the spectral curve within the region of 808 – 920nm displayed the least sensitive to the ripeness. These distinct properties present opportunities for leveraging ripeness assessment in oil palm fruit bunches.

The proposed design of the laser remote sensor incorporated three laser wavelengths (in the range of 550 – 900nm) as illuminating sources. The selection criteria for the first two wavelengths were based on their exceptional sensitivity to FFB ripeness. The reflected power of these two wavelengths had demonstrated a strong correlation with fruit bunch ripeness. The laser operating in the region of 800-900nm was selected as referencing parameter in the measurement.

3. LASER REMOTE SENSOR



Figure 5. The appearance of the laser remote sensor.

The sensor system comprised of three laser modules emitting at distinct wavelengths, each channeled through separate fan-out fibers and consolidated via a 3-to-1 bundled optical fiber into a common output connector. This lens was used to converge the reflected or scattered beam from the targeted fruit to the lens's focal point, where a photodetector detected the focused reflected beam. Notably, a larger lens diameter corresponds to enhanced optical intensity of the collected beam. The laser remote sensor incorporated an Arduino microcontroller for the control of the laser modules, signal acquisition for the reflected intensity from the photodetector, and some basic calculations.

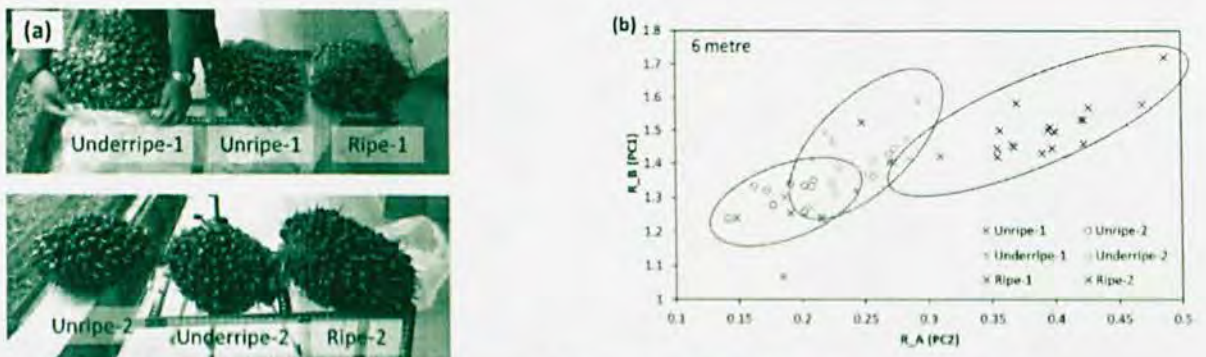


Figure 6. (a) FFBs at different categories of ripeness, and (b) Discriminant analysis plot.

Figure 6(a) shows the experimental results of the laser remote sensor for 6 FFBs of three different categories (Unripe-1, Unripe-2, Underripe-1, Underripe-2, Ripe-1 and Ripe-2). The FFBs were positioned at a distance of 7m from the laser remote sensor. The detected intensities of the reflected beams are calculated, and the results are presented in the discriminant analysis plot in Fig. 6(b). The data from the unripe FFBs are mostly concentrated within the vicinity of (PC1, PC2) \sim (1.25, 0.18) whereas the data of underripe FFBs are at \sim (1.3, 0.21) and ripe FFBs at \sim (1.3 – 1.4, 0.24 – 0.4). Both PC1 and PC2 increase progressively with increasing levels of ripeness of the FFBs. Ripe-1 had lost more fruitlets than Ripe-2 and the thorns of the bunch are more exposed. This explains its high PC2 values.

4. ON TREE ASSESSMENT

In the conventional approach, the assessment of the ripeness of oil palm FFBs primarily relies on visual scrutiny. This approach involves the consideration of various parameters including colouration, bunch dimensions, and the count of loose fruits on the ground. However, this method encounters considerable impediments when deployed for FFBs situated on tall palm trees. Its reliability is contingent upon ambient light conditions and the visibility of FFBs to ground-level observers. As illustrated in Fig. 7(a), images showing an FFB while positioned atop a 7-meter-tall oil palm tree and subsequent to harvesting on the ground are presented. Despite being adjudged underripe upon visual assessment on the tree (Refer Fig. 7(a)), closer scrutiny revealed that it was ripe (Refer Fig. 7(b)). Subsequent analysis encompassing bunch and oil assessments unveiled a notable oil content within this FFB (oil to dry mesocarp ratio, $O/DM = 77.1\%$), contradicting its initial visual classification. Fig. 7(c) and (d) show the on-tree measurement using the proposed instrument. Red laser beam on the FFB marks the points of measurement.

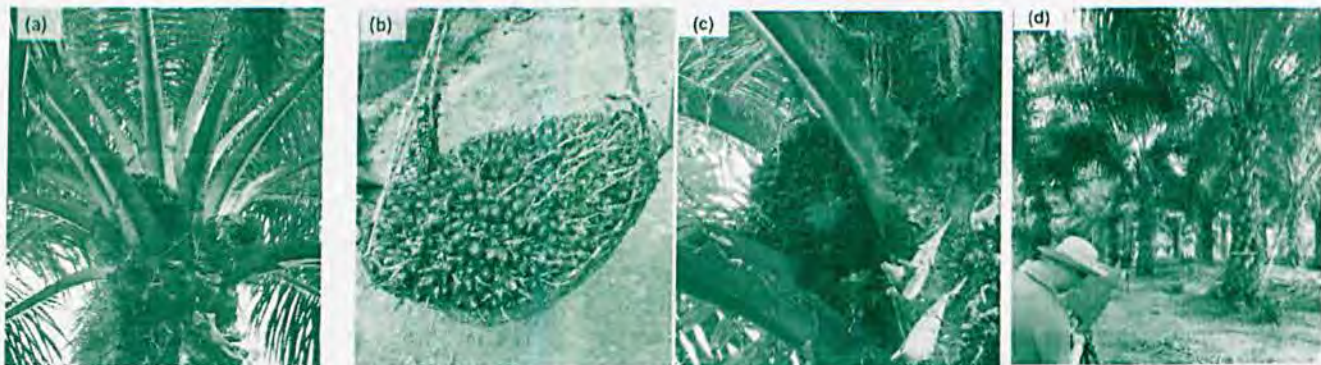


Fig. 7. The appearance of (a) an FFB (red dotted circle) on a 7m tall palm tree and (b) at a closer distance after harvesting (c) Laser beam pointed on FFB (d) On-tree measurement for a 7m height oil palm tree.

The developed laser remote sensor was deployed in Tanah Merah estate, Negeri Sembilan, Malaysia for on-tree assessment. A total of 38 FFBs were assessed and compared against the classifications based on visual inspection and bunch and oil analysis.

5. OPERATION PRINCIPLE AND OIL CONTENT INDEX

The measurement is based on the linear discriminant analysis (LDA). LDA is a supervised technique, utilizes class labels to find a feature combination that best distinguishes between classes. It begins by calculating class means and covariance matrices, computing within-class and between-class scatter matrices. The primary aim is to derive a linear discriminant function that maximizes the ratio of between-class to within-class scatter, enabling optimal class separation. The dataset is then projected onto this function, reducing dimensions while preserving essential discriminative details for tasks like classification. The algorithm for determining the ripeness is given by,

$$L = (R_A - 0.22) + (R_B - 1.3)$$

Where R_A and R_B are the reflectance from two sensing wavelengths. The ripeness classification based on L-value is as follows,

UNRIPE	UNDERRIPE	RIPE
$L < -0.1$	$-0.1 < L < 0$	$L > 0$

Table 1. The ripeness classification of L-value

On the other hand, the oil content parameters of each FFB determine the actual ripeness. The oil content parameter consists of oil to bunch ratio (O/B), oil to dry mesocarp ratio (the mesocarp was dried in oven, O/DW), oil to wet mesocarp ratio (mesocarp was not dried in oven, O/WM) and moisture content (lower moisture indicates more conversation, MC). Table 2 provides the ripeness classification for FFBs.

	UNDERRIPE	RIPE
O/B	below 25%	25% and above
O/DM	below 70%	70% and above
O/WM	below 50%	50% and above
MC	above 40%	below 40%

Table 2. The ripeness classification of oil content parameters.

For simplicity of analysis, oil content index (OCI) is a single value index that describes the oil content of the FBBs and OCI can be constructed as follows,

$$OCI = \left(\frac{O}{B} - 25\right) * W_{\frac{O}{B}} + \left(\frac{O}{DM} - 70\right) * W_{\frac{O}{DM}} + \left(\frac{O}{WM} - 50\right) * W_{\frac{O}{WM}} + (40 - MC) * W_{MC}$$

$$W_{\frac{O}{B}} + W_{\frac{O}{DM}} + W_{\frac{O}{WM}} + W_{MC} = 1$$

where $W_{O/B}$, $W_{O/DM}$, $W_{O/wm}$ and W_{MC} denote the weightages of each oil content parameter in the OCI. Table 3 describes the ripeness classification based on OCI

UNRIPE	UNDERRIPE	RIPE
OCI < -10	-10 < OCI < 0	OCI > 0

Table 3. The ripeness classification of OCI.

6. PERFORMANCE METRICS AND RESULTS

This section delves into key statistical metrics offering insights into classification models, notably featuring the widely utilized confusion matrix. It serves as a vital measure applicable to both binary and multiclass classification problems, presenting predictions in a matrix form. This matrix provides a comprehensive view of correct and incorrect predictions per class, offering valuable clarity on model confusion between different classes. As part of the performance assessment in classification algorithms, the confusion matrix stands out among the preferred parameters, effectively visualizing and summarizing their performance.

It tallies predicted and actual values, distinguishing True Negatives (TN) as accurately classified negatives and True Positives (TP) as accurately classified positives. They also encapsulate False Positives (FP), where actual negatives are misclassified as positives, and False Negatives (FN), where actual positives are misclassified as negatives. Once the confusion matrix is generated for each implemented algorithm the following metric values, accuracy, sensitivity, specificity, and error rate, are calculated from the confusion matrix.

In the ripeness classification which consists of unripe, underripe and ripe, a multiclass classification is more applicable to access the performance evaluation. When there are more than two classes, it expands to represent performance across multiple classes. The structure becomes a square matrix with rows and columns corresponding to the different classes. It provides a more detailed breakdown of a model's performance beyond simple accuracy. It helps in understanding how well a model performs for different classes and aids in identifying specific areas where the model might need improvement. It evaluates the correctness of predictions across multiple classes rather than just two. The goal is to measure how well the model performs for each individual class in a scenario with more than two classes.

The OCI is the gold standard in classifying the ripeness of the FFBs whereas the data from the remote sensor and the visual inspection are the estimations in this study.

(a)	Prediction: Remote sensor		
	Unripe	Underripe	Ripe
Unripe	7	1	3

Actual: OCI standard	Underripe	0	1	5
	Ripe	0	1	20

(b)		Prediction: Visual Inspection		
		Unripe	Underripe	Ripe
Actual: OCI standard	Unripe	8	1	2
	Underripe	1	5	0
	Ripe	6	12	3

Table 4. The confusion matrix of a total 38 FFBS for (a) Remote sensor and (b) Human visual inspection

Based on the confusion matrix in Table 4, accuracy (ACC) can be calculated based on the following expression

$$ACC = \frac{TP + TN}{TP + TN + FP + FN}$$

ACC gauges the accuracy of the laser remote sensor in the ripeness assessment with reference to the oil content data of the fruit samples. Similar accuracy assessment is performed for the data made by human visual inspection. The accuracies of the remote sensor and visual inspection are calculated to be 73.68% and 42.11%, respectively.

7. SUMMARY

A laser remote sensor has been developed and demonstrated ripeness detection for oil palm FFBS. The optical instrument has been tested in the estate, and a total of 38 FFBS have been assessed on the trees at an approximate distance of 7-meter. The superior accuracy of the laser remote sensor (~73.68%) can be attributed to its long working range and strong immunity to the interference of ambient light which varies throughout the day. The laser remote sensor system is finely tuned to the unique spectral characteristics of oil palm FFBS. It has proven to be a practical and efficient tool for non-destructive, precision ripeness assessment. Its adaptability to diverse ripening stages and ability for on-plants of varying heights positions make it a valuable asset for precision harvesting and yield predictions in oil palm plantations. The system's portability enhances its accessibility, offering a solution that can be easily deployed across different locations within oil palm estates for effective and accurate ripeness assessments.

ACKNOWLEDGEMENTS

This work was supported by Sime Darby Plantation Sdn. Bhd., Selangor (PV042-2022).

REFERENCES

- [1] Baltazar, A.; Aranda, J.I.; González-Aguilar, G. Bayesian classification of ripening stages of tomato fruit using acoustic impact and colorimeter sensor data. *Comput. Electron. Agric.* 2008, 60, 113–121
- [2] Choi, K.; Lee, G.; Han, Y.J.; Bunn, J.M. Tomato maturity evaluation using color image analysis. *Trans. ASAE* 1995, 38, 171–176
- [3] Yang, H.Q. Nondestructive Prediction of Optimal Harvest Time of Cherry Tomatoes Using VIS-NIR Spectroscopy and PLSR Calibration. *Adv. Eng. Forum* 2011, 1, 92–96.
- [4] Sivakumar, S.S.; Qiao, J.; Wang, N.; Gariépy, Y.; Raghavan, G.S.V.; McGill, J. Detecting maturity parameters of mango using hyperspectral imaging technique. In *Proceedings of the 2006 ASAE Annual Meeting*, Portland, OR, USA, 9–12 July 2006.